Chapter 5

REACTION MECHANISMS

1

How?

A + B ⟶ C

1

2

REACTION MECHANISMS

rapidly

completely

How?

temperature *light*

environment *solvent*

A + B ⟶ C

2

3

REACTION MECHANISMS

rapidly
completely
How?
temperature
light
environment
solvent

Reactive Intermediate(s) [ ]* [ ]‡ Transition State(s) Further transformations

Reactant rearrangements

3

4

REACTION MECHANISMS

A detailed description of the process leading **from the reactants to the products** of a reaction, including a characterization as complete as possible of the **composition**, **structure**, **energy** and other properties of **reaction intermediates**, **products** and **transition states**. An acceptable mechanism of a specified reaction (and there may be a number of such **alternative** mechanisms not excluded by the evidence) must be consistent with the reaction **stoichiometry**, the **rate law** and with all other available experimental data, such as the **stereochemical** course of the reaction. It should be noted that for many reactions all this information is not available and the suggested mechanism is based on incomplete experimental data.

IUPAC Gold Book

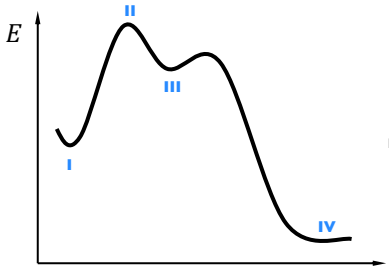

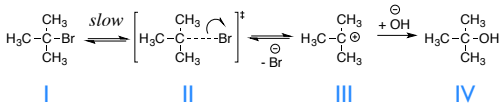

4

Potential Energy Surface (PES)

5

A geometric hypersurface on which the potential **energy** of a chemical system is plotted as a function of its nuclear coordinates (molecular **geometry**).

Chemistry ⟷ *Topology*

5

Potential Energy Surface (PES)

6

A geometric hypersurface on which the potential **energy** of a chemical system is plotted as a function of its nuclear coordinates (molecular **geometry**).

Chemistry ⟷ *Topology*

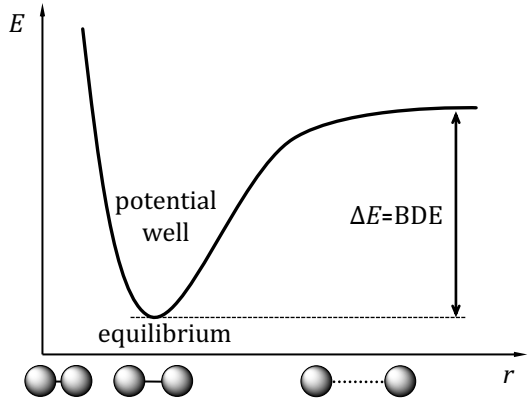

Simplest PES = 1D diagram, e.g. for a diatomic

6

Potential Energy Surface (PES)

7

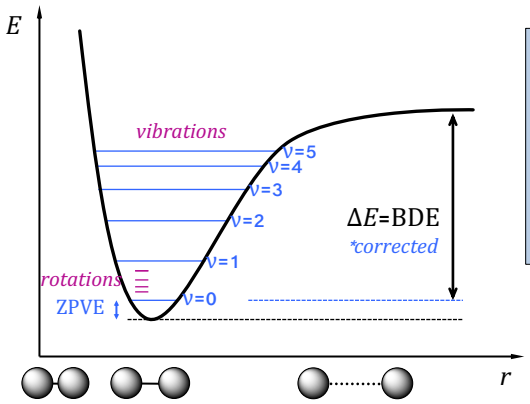

Zero-point vibrational energy (ZPVE)
lowest possible energy of a quantum system. According to the *uncertainty principle*, ZPVE > the minimum of the classical potential well.

7

Potential Energy Surface (PES)

8

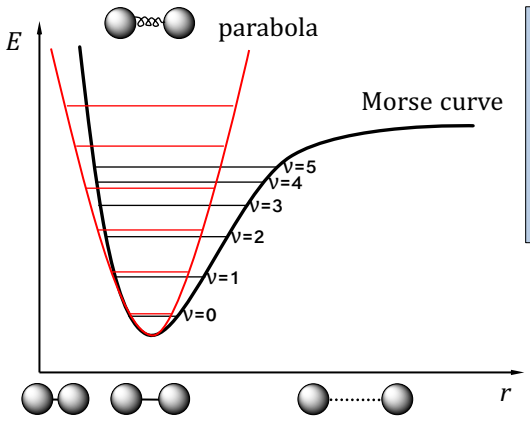

The Harmonic Oscillator approximation
is used to describe vibrational modes at the bottom of the potential well; *Morse curve* is more accurate for higher energies.

8

Potential Energy Surface (PES)

9

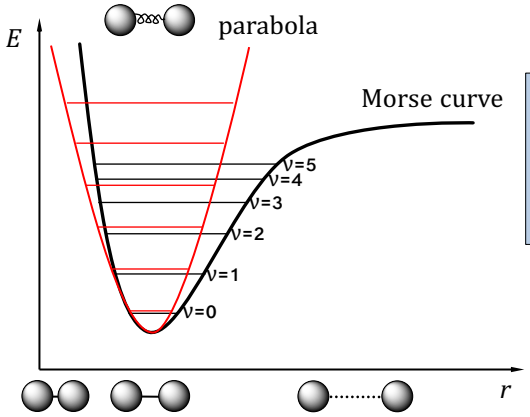

Note that the energy can be given in wavenumbers:
$E = h\nu = hc\overline{\nu}$

$1\ kJ = 5.034 \times 10^{25}\ cm^{-1}$

9

Potential Energy Surface (PES)

10

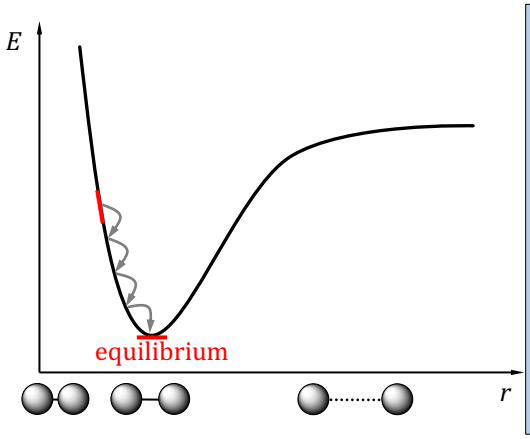

Geometry optimisation is an iterative procedure to reach an equilibrium position by *minimising* the *energy* through geometrical changes. Equilibrium is reached once there is no *force* (-gradient = first derivative of energy = slope of the curve) to shift the nuclei. Equilibrium is the *minimum* of the potential energy well, and corresponds to the zero slope.

10

Potential Energy Surface (PES)

10

Geometry optimisation can be performed using different algorithms to determine the steps towards the energy minimum

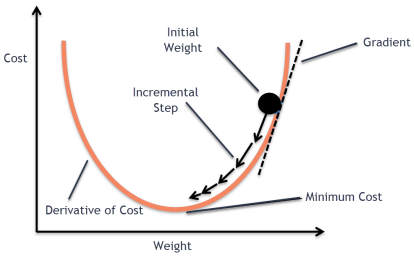

(a)

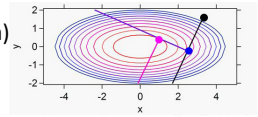

(b)

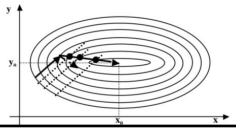

Geometry optimisation

Steepest Descent (a): Brute force, more robust algorithms that improves the choice of the new direction close to the minimum are preferred.

Conjugated Gradient (b): Same as SD at the beginning but subsequent directions are linear combinations of new and previous gradient direction.

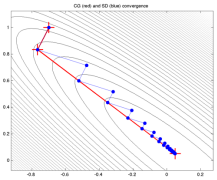

11

Potential Energy Surface (PES)

11

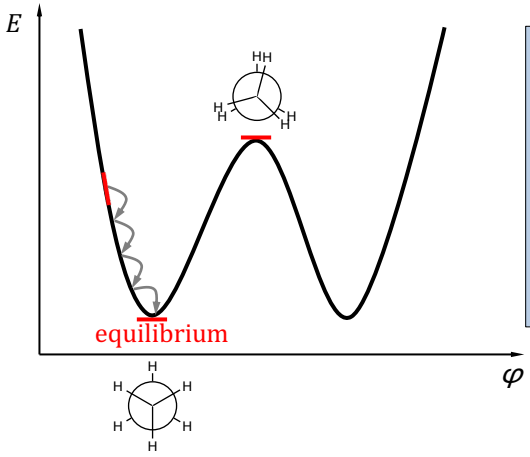

In both the staggered and the eclipse conformations the slope is zero, yet only the staggered is the energy minimum.
For more complicated systems there are more degrees of freedom - need higher dimensionality!

Simplest PES = 1D diagram, e.g., for rotation

12

Potential Energy Surface (PES)

12

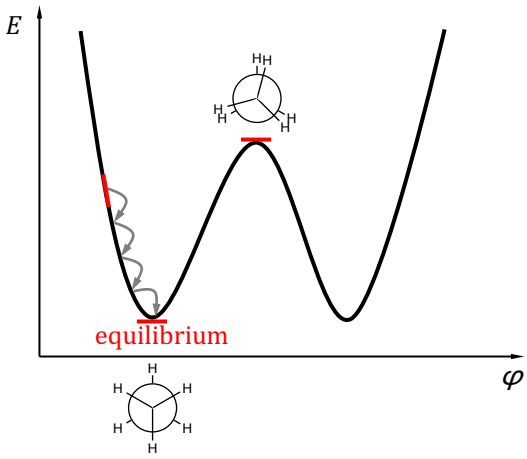

3D surface

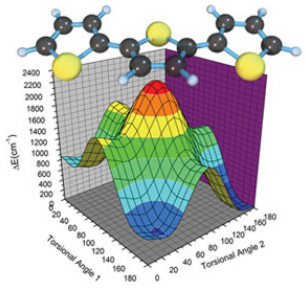

Torsional potential energy of α-terthiophene

13

Potential Energy Surface (PES)

13

Potential energy surface of a molecular system characterises various conformers and bonding patterns, as well as the transition pathways connecting them.

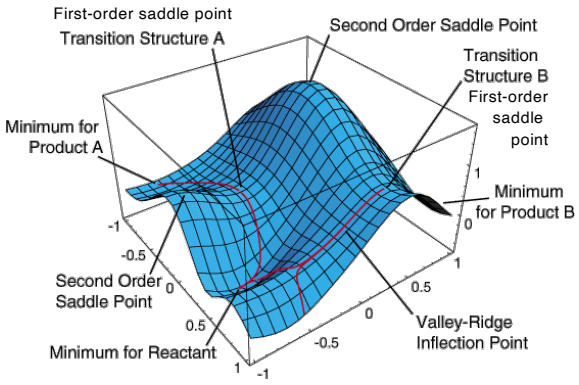

$$\mathbf{A \rightleftharpoons TS_A \rightleftharpoons Reactant \rightleftharpoons TS_B \rightleftharpoons B}$$

14

Potential Energy Surface (PES)

14

Stationary points (force = 0):
Minima (global and local)
Maxima
Transition States (1st order saddle points)
Higher order Saddle Points

Hessian (matrix of the 2nd derivatives of energy) allows distinguishing between them.

Minimum has only positive eigenvalues (vibrational frequencies) in the Hessian;

Saddle point has one negative (imaginary) frequency.

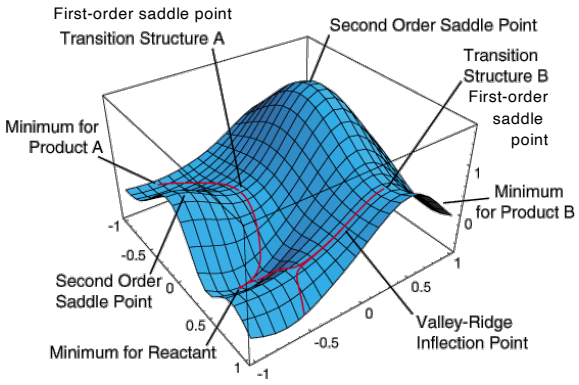

$$A \rightleftharpoons TS_A \rightleftharpoons Reactant \rightleftharpoons TS_B \rightleftharpoons B$$

15

Potential Energy Surface (PES)

15

Geometry optimisation: benchmarking of DFT methods

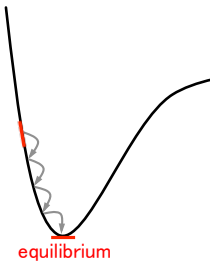

Table 22 Mean errors for bond lengths (Å)

Method	MGBL19		MLBL13		TMBL8		TMBL7	BMUE39[b]	BMUE40[c]
	MSE	MUE	MSE	MUE	MSE	MUE	MUE[a]		
PBE	0.009	0.009	−0.002	0.010	0.016	0.031	0.029	0.016	0.017
TPSSh	0.002	0.004	−0.004	0.010	0.019	0.049	0.047	0.020	0.021
BLYP	0.012	0.012	0.007	0.013	0.034	0.039	0.041	0.022	0.022
M06-L	−0.001	0.003	−0.001	0.011	0.101	0.118	0.043	0.019	0.044
VSXC	0.003	0.003	0.008	0.013	0.119	0.138	0.037	0.018	0.052
M06	−0.005	0.007	−0.007	0.018	0.112	0.131	0.056	0.027	0.052
B3LYP	0.000	0.005	−0.003	0.010	0.126	0.154	0.057	0.024	0.057
M05	−0.005	0.007	−0.001	0.021	0.134	0.154	0.071	0.033	0.061
B98	−0.001	0.005	0.001	0.011	0.156	0.174	0.086	0.034	0.063
PBEh	−0.004	0.006	−0.010	0.014	0.129	0.173	0.061	0.027	0.064
BMK	−0.004	0.007	−0.011	0.025	0.161	0.183	0.075	0.036	0.072
B97-3	−0.004	0.006	0.009	0.018	0.175	0.197	0.095	0.040	0.074
M05-2X	−0.008	0.009	0.005	0.023	0.174	0.213	0.113	0.048	0.082
M06-2X	−0.006	0.007	0.006	0.037	0.202	0.244	0.143	0.062	0.096
M06-HF	−0.011	0.012							
HFLYP	−0.033	0.033							
HF	−0.022	0.035							
Average (DFT)	−0.003	0.008	0.000	0.017	0.118	0.143	0.068	0.030	0.055
Average (all)	−0.005	0.010							

The MG3S basis set is employed for the MGBL19 database, and the TZQ basis set is employed for the MLBL13 and TMBL databases
[a] This MUE excludes the bond length of Cr_2
[b] BMUE39 = (MUE(MGBL19) + MUE(MLBL13) + MUE(TMBL7))/3
[c] BMUE40 = (MUE(MGBL19) + MUE(MLBL13) + MUE(TMBL8))/3

Zhao, Truhlar, *Theor. Chem. Acc.* **2008**, *120*, 215.

16

Potential Energy Surface (PES)

16

Frequency computation is more expensive and can be performed:

- Analytically (available in most common DFT and some post-HF methods)
- Numerically

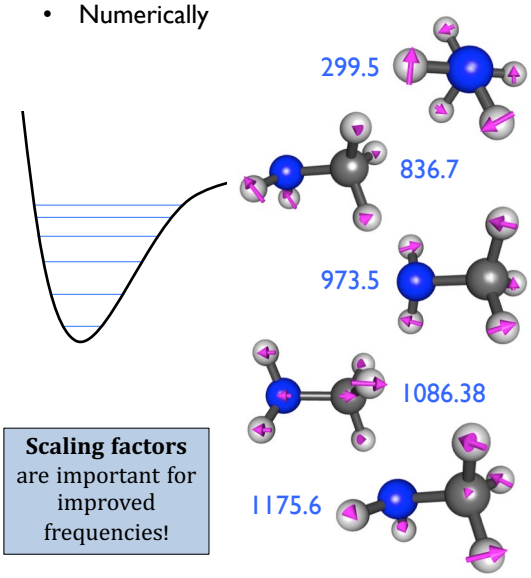

H_2N-CH_3

M06-2X/6-311++G(3df,2p)
frequencies, in cm^{-1}

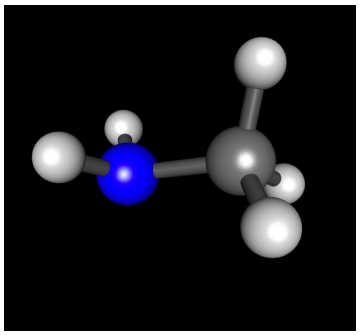

Scaling factors are important for improved frequencies!

17

Potential Energy Surface (PES)

17

Frequency computation is more expensive and can be performed:

- Analytically (available in most common DFT and some post-HF methods)
- Numerically

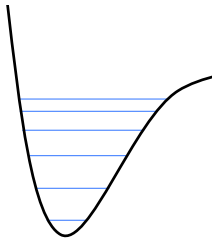

Table 24 Scaling factors for the predictions of harmonic frequencies and zero-point vibrational energies

Method	Frequencies (cm^{-1})			Zero-point energies (kcal/mol)			BMUE[a] (kcal/mol)	
	Scaling factor	MUE		Scaling factor	MUE			
		No scaling	Scaling		No scaling	Scaling	No scaling	Scaling
VSXC	1.001	24	24	0.989	0.13	0.08	0.10	0.07
PBE	1.025	56	29	1.012	0.13	0.08	0.15	0.08
B98	0.995	32	30	0.984	0.19	0.08	0.14	0.08
TPSSh	1.002	28	28	0.986	0.15	0.09	0.11	0.08
BLYP	1.031	67	25	1.016	0.17	0.09	0.18	0.08
B3LYP	0.998	31	31	0.985	0.17	0.08	0.13	0.09
B97-3	0.986	46	34	0.974	0.29	0.09	0.21	0.09
M06-L	0.996	39	36	0.980	0.21	0.10	0.16	0.10
BMK	0.984	52	42	0.973	0.32	0.09	0.23	0.11
PBEh	0.989	46	39	0.978	0.27	0.10	0.20	0.11
M05	0.989	54	49	0.979	0.26	0.12	0.21	0.13
M05-2X	0.975	72	45	0.964	0.41	0.13	0.31	0.13
M06-2X	0.982	57	47	0.972	0.34	0.13	0.25	0.13
M06	0.994	60	59	0.983	0.23	0.16	0.20	0.16
HF	0.932	180	69	0.921	0.93	0.20	0.72	0.20
M06-HF	0.967	95	68	0.957	0.49	0.22	0.38	0.20
HFLYP	0.912	233	74	0.902	1.17	0.22	0.92	0.21
Average (DFT)		67	41		0.34	0.12	0.26	0.12
Average (all)		69	43		0.35	0.12	0.27	0.12

The MG3S basis set is employed for all calculations in this table

[a] BMUE = (MUE(F38/06, in kcal/mol)) + MUE(ZPVE15/06))/2. Note that 1 kcal/mol = 349.75 cm^{-1}

Zhao, Truhlar, *Theor. Chem. Acc.* **2008**, *120*, 215.

Scaling factors are important for improved frequencies!

18

Potential Energy Surface (PES)

18

Transition states are characterized with one imaginary frequency that corresponds to the direction of chemical transformation.

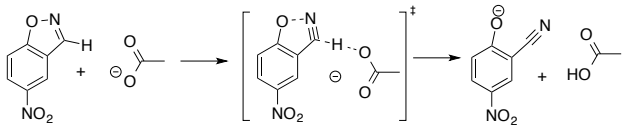

barrier width

$$\Delta = \frac{1}{\omega^{\ddagger}}$$

imaginary frequency

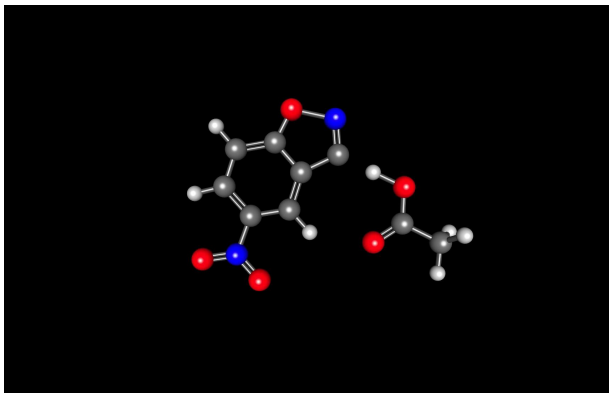

Frequencies are important, especially the single negative one!

M06-2X/6-31+G(d), 564*i* cm^{-1}

19

Potential Energy Surface (PES)

19

Transition states are characterized with one imaginary frequency that corresponds to the direction of chemical transformation.

barrier width

$$\Delta = \frac{1}{\omega^{\ddagger}}$$

imaginary frequency

Table 4. Effect of level of theory on the imaginary frequency (cm^{-1}) for the hydrogen abstraction reactions $\bullet CH_2X + CH_3Y \rightarrow CH_3X + \bullet CH_2Y$.[a]

	Reaction: $\bullet CH_2X + CH_3Y \rightarrow CH_3X + \bullet CH_2Y$				
	X,Y = H,H	X,Y = H,CN	X,Y = H,F	X,Y = H,Li	X,Y = F,Li
Level of theory	(1)	(2)	(3)	(4)	(5)
RHF/6-31G(d)	3489i (*0.53*)	3376i (*0.55*)	3592i (*0.54*)	3338i (*0.47*)	3418i (*0.31*)
RHF/6-311G(d,p)	3411i (*0.55*)	3315i (*0.56*)	3529i (*0.55*)	3274i (*0.48*)	3376i (*0.31*)
RHF/6-311+G(3df,2pd)	3398i (*0.55*)	3309i (*0.56*)	3528i (*0.55*)	3257i (*0.48*)	3389i (*0.31*)
UHF/6-31G(d)	2558i (*0.73*)	2578i (*0.72*)	2611i (*0.74*)	2421i (*0.65*)	2096i (*0.50*)
UHF/6-311G(d,p)	2518i (*0.74*)	2537i (*0.73*)	2572i (*0.75*)	2382i (*0.66*)	2070i (*0.51*)
UHF/6-311+G(3df,2pd)	2530i (*0.74*)	2545i (*0.73*)	2585i (*0.74*)	2397i (*0.66*)	2110i (*0.50*)
RB3-LYP/6-31G(d)	1741i (*1.07*)	1658i (*1.12*)	1760i (*1.09*)	1368i (*1.15*)	796i (*1.31*)
RB3-LYP/6-311G(d,p)	1713i (*1.09*)	1640i (*1.13*)	1739i (*1.11*)	1358i (*1.16*)	832i (*1.26*)
RB3-LYP/6-311+G(3df,2pd)	1725i (*1.08*)	1656i (*1.12*)	1770i (*1.09*)	1392i (*1.13*)	926i (*1.13*)
UB3-LYP/6-31G(d)	1657i (*1.13*)	1592i (*1.17*)	1673i (*1.15*)	1311i (*1.20*)	737i (*1.42*)
UB3-LYP/6-31G(2df,p)	1638i (*1.14*)	1568i (*1.19*)	1649i (*1.17*)	1286i (*1.22*)	674i (*1.55*)
UB3-LYP/6-311G(d,p)	1638i (*1.14*)	1579i (*1.18*)	1659i (*1.16*)	1306i (*1.20*)	790i (*1.32*)
UB3-LYP/6-311+G(3df,2pd)	1657i (*1.13*)	1602i (*1.16*)	1697i (*1.13*)	1352i (*1.16*)	891i (*1.17*)
UMPW1K/6-31+G(d,p)	1773i (*1.05*)	1739i (*1.07*)	1824i (*1.05*)	1456i (*1.08*)	827i (*1.26*)
UMP2/6-31G(d)	2134i (*0.87*)	2061i (*0.90*)	2197i (*0.88*)	1849i (*0.85*)	1358i (*0.77*)
UMP2/6-311G(d,p)	1959i (*0.95*)	1865i (*1.00*)	2050i (*0.94*)	1600i (*0.98*)	1221i (*0.86*)
UMP2/6-311+G(3df,2pd)	1941i (*0.96*)	1829i (*1.02*)	2038i (*0.94*)	1569i (*1.00*)	1185i (*0.88*)
UCCSD(T)/6-31G(d)	2029i (*0.92*)	2010i (*0.93*)	2073i (*0.93*)	1765i (*0.89*)	1126i (*0.93*)
UCCSD(T)/6-311G(d,p)	1866i (*1*)	1859i (*1*)	1924i (*1*)	1574i (*1*)	1046i (*1*)

[a] The numbers in parentheses are the scale factors required to convert the imaginary frequency into the corresponding CCSD(T)/6-311G(d,p) value.

Frequencies are important, especially the single negative one!

Coote, Collins, Radom, *Mol. Phys.* **2003**, *101*, 1329.

20

Potential Energy Surface (PES)

20

No experimental benchmark exists for TS structures

Table 3. The Average Mean Unsigned Deviations (AMUD, in Å) of Transition State Geometries Obtained Using 36 Model Chemistries, Compared to the TSG48 Database

method	type[a]	HTG9	HATG9	NSG9	UAG9	MHTG12	**TSG48**	TSG39[b]
QCISD/MG3	WFT	0.020	0.013	0.015	0.014	0.014	**0.015**	0.014
MP2/MG3S	WFT	0.038	0.067	0.017	0.041	0.025	**0.037**	0.034
MC3BB	DHDFT	0.011	0.020	0.009	0.018	0.009	**0.013**	0.013
M08-HX/MG3S	H-m	0.016	0.012	0.013	0.016	0.014	**0.014**	0.015
MC3MPW	DHDFT	0.012	0.027	0.012	0.023	0.009	**0.016**	0.015
M06-2X/MG3S	H-m	0.021	0.013	0.017	0.025	0.012	**0.017**	0.018
M08-SO/MG3S	H-m	0.018	0.022	0.030	0.017	0.020	**0.021**	0.020
ωB97/MG3S	H	0.030	0.025	0.013	0.034	0.011	**0.022**	0.023
PWB6K/MG3S	H-m	0.028	0.022	0.015	0.031	0.021	**0.023**	0.024
B2PLYP/MG3S	DHDFT	0.019	0.029	0.042	0.017	0.015	**0.024**	0.018
BB1K/MG3S	H-m	0.030	0.024	0.014	0.038	0.018	**0.025**	0.025
ωB97X/MG3S	H	0.034	0.026	0.014	0.040	0.013	**0.025**	0.025
MPWB1K/MG3S	H-m	0.029	0.022	0.018	0.037	0.019	**0.025**	0.026
M05-2X/MG3S	H-m	0.041	0.022	0.015	0.056	0.006	**0.027**	0.028
BMK/MG3S	H-m	0.034	0.039	0.013	0.039	0.016	**0.028**	0.027
MPW1K/MG3S	H	0.029	0.021	0.018	0.058	0.017	**0.028**	0.030
ωB97X-D/MG3S	H	0.036	0.035	0.021	0.046	0.015	**0.030**	0.029
BHandHLYP/MG3S	H	0.043	0.023	0.023	0.051	0.021	**0.032**	0.031
M06-HF/MG3S	H-m	0.044	0.019	0.045	0.030	0.032	**0.034**	0.035
PW6B95/MG3S	H-m	0.038	0.048	0.025	0.045	0.021	**0.034**	0.030
PBE0/MG3S	H	0.037	0.041	0.016	0.068	0.023	**0.036**	0.033
M06/MG3S	H-m	0.044	0.047	0.033	0.051	0.016	**0.037**	0.033
mPW1PW/MG3S	H	0.036	0.042	0.021	0.068	0.022	**0.037**	0.033
TPSS25B95/MG3S	H-m	0.048	0.050	0.032	0.043	0.024	**0.038**	0.031
B97-3/MG3S	H	0.039	0.045	0.034	0.053	0.024	**0.038**	0.035
M05/MG3S	H-m	0.042	0.048	0.041	0.078	0.021	**0.044**	0.040
B98/MG3S	H	0.058	0.076	0.047	0.071	0.028	**0.054**	0.046
B1LYP/MG3S	H	0.059	0.071	0.066	0.069	0.024	**0.056**	0.049
B3LYP/MG3S	H	0.065	0.095	0.069	0.080	0.029	**0.065**	0.054
M06-L/MG3S[c]	m	0.070	0.100	0.069	0.081	0.039	**0.070**	0.057
rHCTHhyb/MG3S[c]	H-m	0.084	0.107	0.059	0.087	0.040	**0.073**	0.058
SOGGA/MG3S[d]	GGA	0.132	0.032	0.043	0.159	0.069	**0.086**	0.091
MOHLYP2/MG3S	GGA	0.074	0.101	0.199	0.056	0.072	**0.099**	0.082
BLYP/MG3S[c,d,e]	GGA	0.163	0.125	0.148	0.133	0.065	**0.123**	0.108
MOHLYP/MG3S[c,d]	GGA	0.205	0.117	0.126	0.137	0.076	**0.129**	0.121
B97-D/MG3S[c,d,e]	H	0.285	0.117	0.149	0.168	0.054	**0.148**	0.140

[a] Abbreviations: WFT, wave function theory; DHDFT, doubly hybrid DFT; H-m, hybrid meta-GGA; H, hybrid GGA; m, meta-GGA; GGA, generalized gradient approximation. [b] TSG39 is the same as TSG48 except that R6, R8, and R15 are omitted. [c] The transition state of reaction R6 cannot be located. The largest deviations of the three key bond lengths obtained using other model chemistries were used to calculate the MUD in such cases. [d] The transition state of reaction R15 cannot be located. The largest deviations of the three key bond lengths obtained using other model chemistries were used to calculate the MUD in such cases. [e] The transition state of reaction R8 cannot be located. The largest deviations of the three key bond lengths obtained using other model chemistries were used to calculate the MUD in such cases.

Xu, Alecu, Truhlar, *J. Chem. Theory. Comput.* **2011**, *7*, 1667.

21

Potential Energy Surface (PES)

21

Geometry optimisation can be performed using different algorithms to determine the steps towards the energy minimum

Transition states cannot be observed experimentally! Computationally they can be located using logical guess geometry or other search algorithms.

Multiple Local minima can be located using the following algorithms:

- Monte-Carlo (randomization-minimization)
- Molecular dynamics, including simulated annealing
- Enhanced sampling (REMD, …)
- Genetic algorithms
- Distance geometry
- Systematic conformational search in torsional and Cartesian space, Eigenvector-following

22

Potential Energy Surface (PES)

See it all with brut-force global reaction route mapping (GRRM)

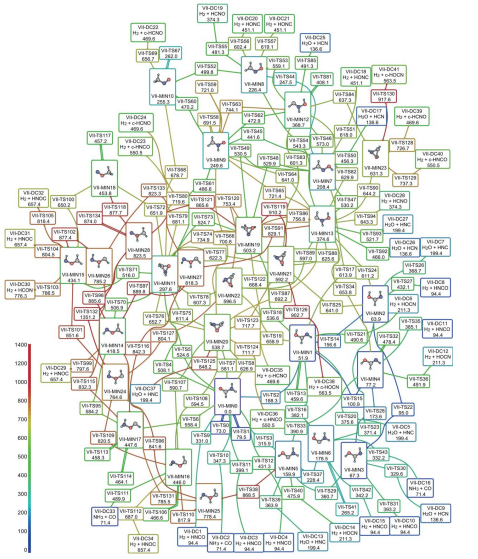

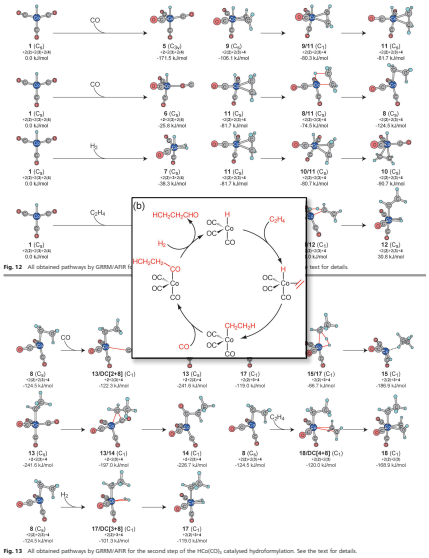

Figure 7. An IRC network for whole of the PES of CH_2NO obtained by the SC-AFIR method. Colors of structure flames and connection lines follow the color code which varies depending on energy values.

Morokuma et al, *Int. J. Quantum Chem.* **2015**, *115*, 258.

Morokuma et al, *Phys. Chem. Chem. Phys.* **2013**, *15*, 3683.

23

Potential Energy Surface (PES)

Temperature as another computational trick to explore the PES

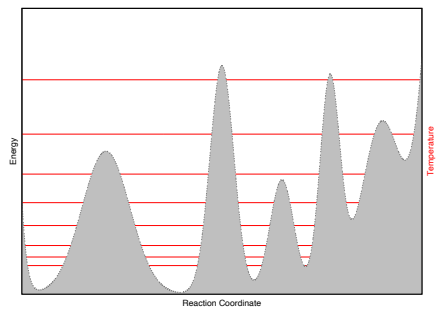

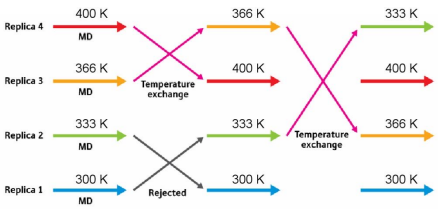

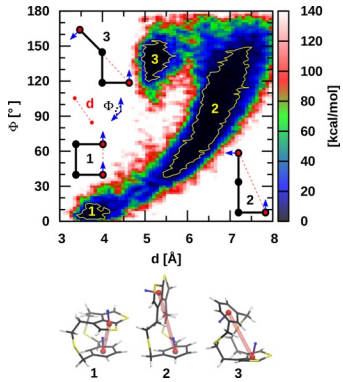

Molecular dynamic trajectories exchanging their temperatures

Replica Exchange Molecular Dynamics
Sugita and Okamoto, *Chem. Phys. Lett.* **1999**, *314*, 141.

Corminboeuf et al, *J. Chem. Comp.* **2016**, *37*, 83.

24

Reaction Energy Profile

23

Meaningful insight into the reaction mechanism does not require exploring the full PES – only the *plausible* minima and the most *energetically preferred* transition states connecting them.

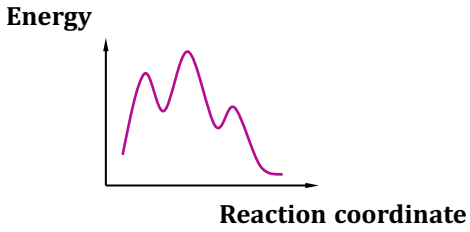

25

Reaction Energy Profile

24

Energy

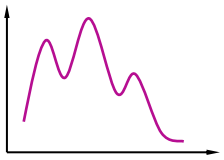

Reaction coordinate

- breaking/forming bond length
- torsional angle
- quasi-chemical index
- reaction sequence progression

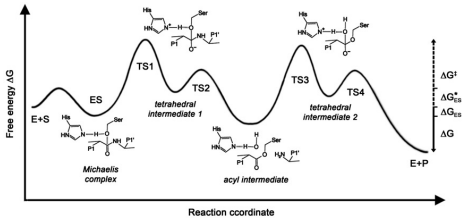

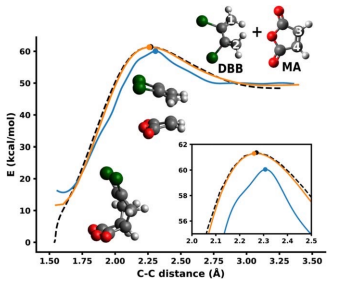

2,3-dibromo-1,3-butadiene and maleic anhydride

26

Reaction Energy Profile

25

$\Delta E = \Delta\varepsilon_0$ -> **always computed**
ε_0 = *electronic energy*

$\varepsilon_0 + \varepsilon_{ZPE}$ = *electronic energy + zero point energy*

$\varepsilon_0 + E_{tot}$ = *electronic energy + thermal energies*
$E_{tot} = E_{trans} + E_{rot} + E_{vib}$

$$\Delta H^T = \Delta(\varepsilon_0 + \varepsilon_{ZPE}) + \\ + \Delta(E^T_{trans} + E^T_{rot} + E^T_{vib})$$

often computed

$$\Delta G^T_{gas} = \Delta H^T_{gas} + T\Delta S^T_{gas}$$
$$\Delta S^T = \Delta(S^T_{trans} + S^T_{rot} + S^T_{vib} + S^T_{elec})$$

often computed

$$\Delta G^T_{soln} = \Delta G^T_{gas} + \Delta\Delta G^T_{solv}$$

often computed

*the more realistic Gibbs's free energy (ΔG) accounts for thermal and Intrinsic entropic contribution from *static* computations.

27

Reaction Energy Profile

	ΔE	ZPE Corr.	ΔH Corr.	ΔG Corr.	Total Gibb's Free Energy
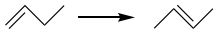	-1.7	-0.6	-0.2	0.6	-1.9
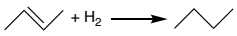	-39.4	8.9	-1.5	8.1	-23.9

Electronic Energy (ΔE)
ZPE Corrected Electronic Energy (ΔE + ZPE Corr.)
Enthalpy (ΔE + ZPE Corr. + ΔH Corr.)
Gibb's Free Energy (ΔE + ZPE Corr. + ΔH Corr. + ΔG Corr.)

The difference between ΔE and ΔG can be significant (*e.g.,* hydrogenation) or negligible (*e.g.*, isomerization) !

Computations at PBE0-D3(BJ)/def2-SVP level
Values in kcal/mol

28

Reaction Energy Profile

	ΔG (Gas Phase)	ΔG (in Solvent)
$CO_2 + H_2 + OH(-) \rightarrow HCOO(-) + H_2O$	-67.6	-46.0 (H_2O)
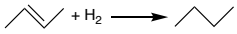	-23.9	-26.4 (CH_2Cl_2)

The difference between ΔG_{gas} and ΔG_{soln} is especially significant in the presence of charged species with polar continuum.

Computations at PBE0-D3(BJ)/def2-SVP level
Values in kcal/mol

29

Reaction Energy Profile

26

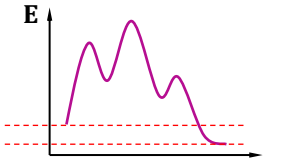

Thermodynamics

$$\Delta G = \Delta H - T\Delta S$$

$$\Delta G < 0$$

$$K_{eq} = \frac{[products]^p}{[reactants]^q} = \exp\left(\frac{-\Delta G^T}{RT}\right)$$

30

Reaction Energy Profile

27

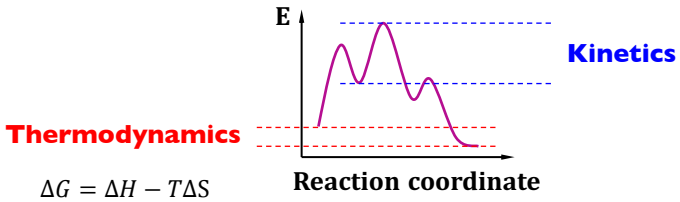

$\Delta G = \Delta H - T\Delta S$

$\Delta G < 0$

$$K_{eq} = \frac{[products]^p}{[reactants]^q} = \exp\left(\frac{-\Delta G^T}{RT}\right) = \frac{k_{fwd}}{k_{rev}}$$

$\Delta G = \Delta G^{\ddagger}_{rev} - \Delta G^{\ddagger}_{fwd}$

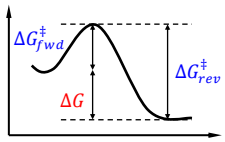

31

Reaction Energy Profile

28

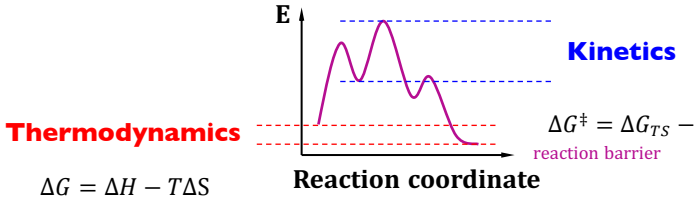

$\Delta G^{\ddagger} = \Delta G_{TS} - \Delta G_{pre-complex}$

reaction barrier

$\Delta G = \Delta H - T\Delta S$

$\Delta G < 0$

$$k = \frac{k_B T}{h}\exp\left(\frac{-\Delta G^{\ddagger}}{RT}\right)$$

rate constant

$$K_{eq} = \frac{[products]^p}{[reactants]^q} = \exp\left(\frac{-\Delta G^T}{RT}\right) = \frac{k_{fwd}}{k_{rev}}$$

$\Delta G = \Delta G^{\ddagger}_{rev} - \Delta G^{\ddagger}_{fwd}$

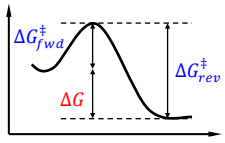

$$\frac{d[X]_t}{dt} = f(k_i, C_{0,i})$$

rate law for species X

32

Reaction Energy Profile

29

Table 9 Mean errors for thermochemical kinetics

Methods	HATBH12		NSBH16		UABH10		Hydrogen Transfer (38)		AMUE	DBH76
	MSE	MUE	MSE	MUE	MSE	MUE	MSE	MUE		BMUE
M06-2X	−0.81	1.61	0.77	1.22	0.32	0.92	−0.51	1.13	1.06	1.22
BMK	−1.21	1.49	0.75	0.91	0.80	1.58	−0.82	1.32	1.29	1.32
M05-2X	1.15	2.00	−0.79	1.48	0.91	1.77	−0.39	1.34	1.39	1.65
B97-3	−2.41	2.41	−0.24	0.80	0.57	1.42	−2.11	2.27	1.48	1.72
M05	−2.84	3.79	0.00	0.80	0.69	2.24	−1.20	1.93	2.06	2.19
M06	−3.33	3.38	−1.53	1.78	0.04	1.69	−1.94	2.00	1.88	2.21
M06-HF	1.79	4.39	−0.71	1.61	0.54	1.45	1.14	2.06	2.22	2.38
B98	−5.18	5.18	−2.96	2.96	−0.31	1.97	−4.16	4.16	2.41	3.57
PBEh	−6.62	6.62	−1.87	2.05	−0.58	2.16	−4.22	4.22	2.75	3.76
M06-L	−5.58	5.93	−3.58	3.58	0.04	1.86	−4.14	4.16	3.02	3.88
B3LYP	−8.49	8.49	−3.25	3.25	−1.42	2.02	−4.13	4.23	3.08	4.50
VSXC	−7.44	7.44	−5.30	5.30	−0.91	2.40	−4.86	4.87	3.45	5.00
TPSSh	−11.51	11.51	−5.78	5.78	−2.94	3.23	−5.97	5.97	4.57	6.62
HFLYP	9.67	11.96	5.26	5.33	3.13	3.54	6.42	7.22	4.77	7.01
HF	14.86	16.87	6.67	6.67	2.70	3.82	1.83	6.28	7.19	8.41
BLYP	−14.66	14.66	−8.40	8.40	−3.38	3.51	−7.52	7.52	5.67	8.52
PBE	−14.93	14.93	−6.97	6.97	−2.94	3.35	−9.32	9.32	5.65	8.64
Average (DFT)	−4.52	6.61	−2.16	3.26	−0.34	2.19	−2.73	3.98	2.92	4.01
Average (all)	−3.38	7.22	−1.64	3.46	−0.16	2.29	−2.46	4.12	3.17	4.27

The QCISD/MG3 geometries and MG3S basis set are used for calculations in this table
AMUE is defined in as: AMUE = [MUE(ΔE,38) + MMUE)/2, where MUE(ΔE,38) is the mean unsigned error for the energy of reactions for the 38 reactions involved in this table. AMUE is one measure of the quality of a method for kinetics
BMUE denotes balanced mean unsigned error (kcal/mol). BMUE for DBH76 is calculated by averaging the numbers in columns 3, 5, 7, and 9; this weighs each of the four component databases equally, so that their contributions are balanced even though they have different numbers of data

Kinetics

$$\Delta G^{\ddagger} = \Delta G_{TS} - \Delta G_{pre-complex}$$

Barrier heights are strongly underestimated/overestimated by GGA/HF.
Hybrid functionals are much better.

Zhao, Truhlar, *Theor. Chem. Acc.* **2008**, *120*, 215.

33

Reaction Energy Profile

30

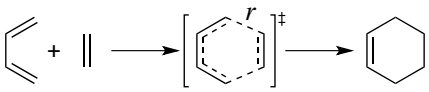

Kinetics

$$\Delta G^{\ddagger} = \Delta G_{TS} - \Delta G_{pre-complex}$$

Method	r, Å	E_a, kcal mol^{-1}
HF/6-31G(d,p)	2.273	45.9
CASSCF(6,6)/6-31(d,p)	2.221	44.5
MR-AQCC/6-31G(d,p)	2.236	25.3
MP2/6-31G(d,p)	2.244	15.9
B3LYP/6-31G(d,p)	2.268	22.4
MPW1K/6-31+G(d,p)		24.4
M06-2X/cc-pVTZ	2.239	23.2
ωB97X-D/cc-pVTZ	2.236	25.1
CCSD(T)/6-311G(d,p)*		25.7
G2MP2/6-311+G(3df,2p)		24.6
CBS-QB3		22.9
Estimated		**23.3±2**

*on a B3LYP/6-31G geometry

Thermodynamics

$$\Delta G = \Delta H - T\Delta S$$

Method	ΔE_{rxn}, kcal mol^{-1}
HF/6-31+G(d,p)	-30.5
MP2/6-31+G(d,p)*	-45.4
B3LYP/6-31+G(d,p)	-31.3
mPW1PW91/6-31+G(d,p)	-40.3
M06-2X/cc-pVTZ	-39.6
ωB97X-D/cc-pVTZ	-41.1
G3	-37.8
CBS-QB3	-38.3
Experiment	**-37.6±0.5**

*on a B3LYP/6-31+G(d,p) geometry

34

Reaction Energy Profile

31

Kinetic control & **Thermodynamic control**

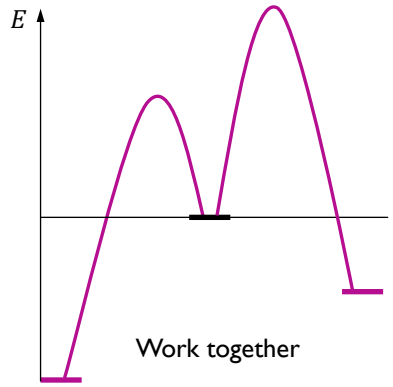

Bell-Evans-Polanyi Principle

$$E_a = A + B\Delta H_r$$

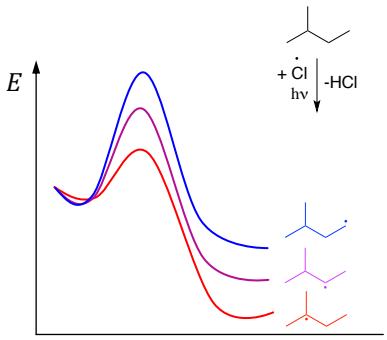

35

Reaction Energy Profile

32

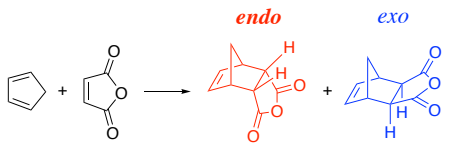

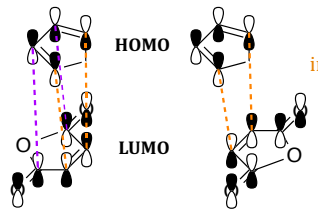

primary orbital interactions

secondary orbital interactions

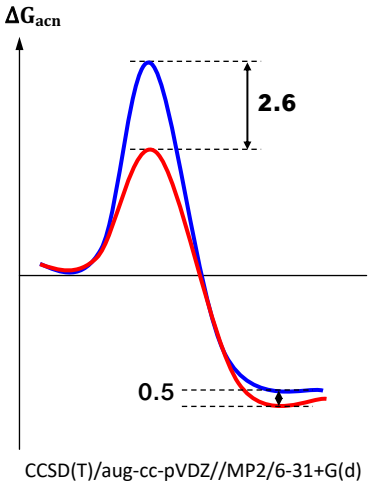

CCSD(T)/aug-cc-pVDZ//MP2/6-31+G(d)

Stavos et al., *J. Org. Chem.* **2005**, *70*, 6295.

36

Reaction Energy Profile

33

Olefin Metathesis

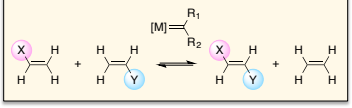

Dissociative mechanism

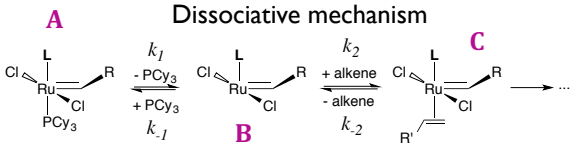

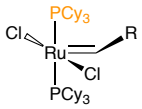

1st gen. k_1 = 0.3 s^{-1} k_{-1}/k_2 = 15300

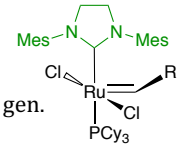

2nd gen. k_1 = 0.003 s^{-1} k_{-1}/k_2 = 1.25

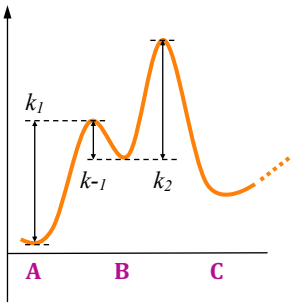

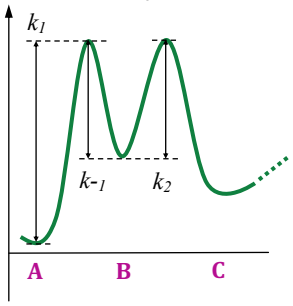

Sunford, Ulman, Grubbs, *J. Am. Chem. Soc.* **2001,** *123,* 749; Bernardi, Bottoni, Miscione, *Organometallics* **2003,** *22,* 940.

37

Reaction Energy Profile

34

Kinetic control ***vs.*** **Thermodynamic control**

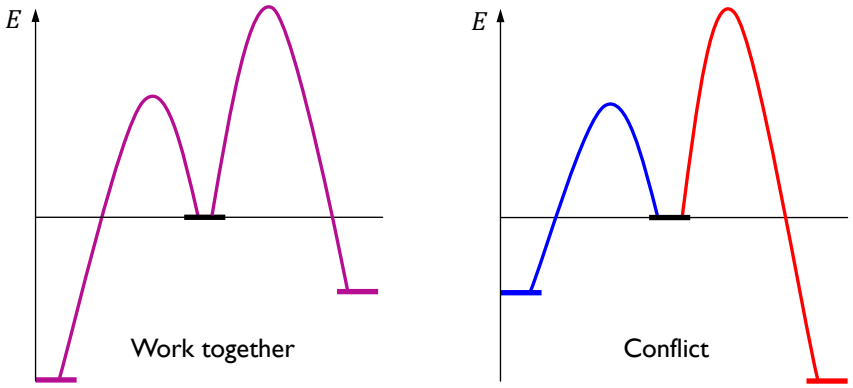

38

Reaction Energy Profile

35

Kinetic control ***vs.*** **Thermodynamic control**

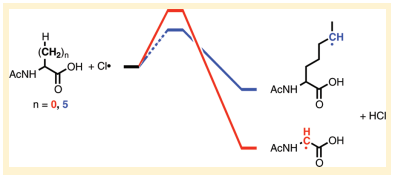

H-abstraction by Cl•

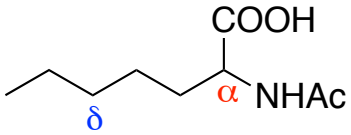

position	experiment (relative rates)	Calculated energies at 298 K in kJ mol^{-1}	
		thermodynamics (ΔG_{soln})	kinetics ($\Delta G^{\ddagger}_{soln}$)
α	≤0.20	-82.0	31.3
δ	5.0	-33.2	23.0

Radom et al., *J. Am. Chem. Soc.* **2011**, *133*, 16553.

B2K-PLYP/A'VTZ//B2K-PLYP/6-31+G(3df,2d,2p)

39

Reaction Energy Profile

36

H-abstraction by Cl•

Kinetic control ***vs.*** **Thermodynamic control**

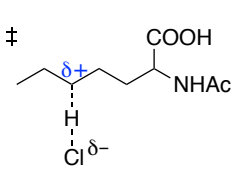

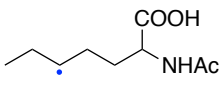

Kinetics: not destabilized

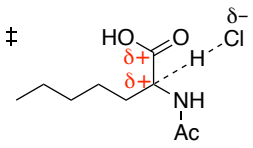

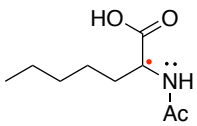

Thermodynamics: stability of the forming C-centered radical

Kinetics: ionic contributor to TS is destabilised by the strong *electron acceptor* COOH group

40

Beyond Transition State Theory

37

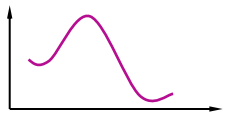

Transition State Theory

$$A + B \rightleftharpoons TS^{\ddagger} \longrightarrow \text{Products}$$

$$k = \frac{k_B T}{h} \exp\left(\frac{-\Delta G^{\ddagger}}{RT}\right)$$

41

Beyond Transition State Theory

38

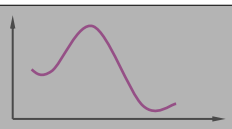

Transition State Theory

$$A + B \rightleftharpoons TS^{\ddagger} \longrightarrow \text{Products}$$

$$k = \frac{k_B T}{h} \exp\left(\frac{-\Delta G^{\ddagger}}{RT}\right)$$

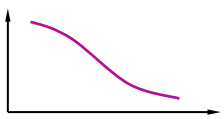

Barrierless

- Radical-radical reactions
- Ion-molecule reactions
- Chelotropic reactions (esp. carbene addition to double bonds)

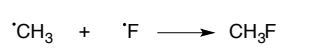

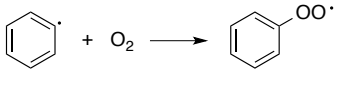

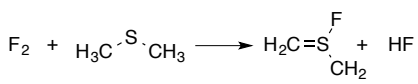

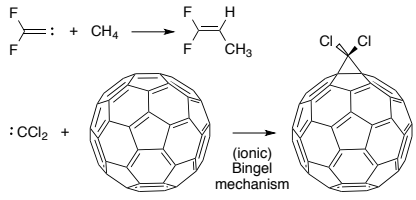

Jasper, Klippenstein, Harding, *J. Phys. Chem. A* **2010**, *114*, 5759.
Tokmakov et al., *J. Phys. Chem. A* **2005**, *109*, 6114.
Kötting, Sander, *J. Am. Chem. Soc.* **1999**, *121*, 8891.
Chen et al., *J. Phys. Chem. A* **2009**, *113*, 3673.
Lin et al., *J. Chem. Phys.* **2007**, *127*, 101101.

42

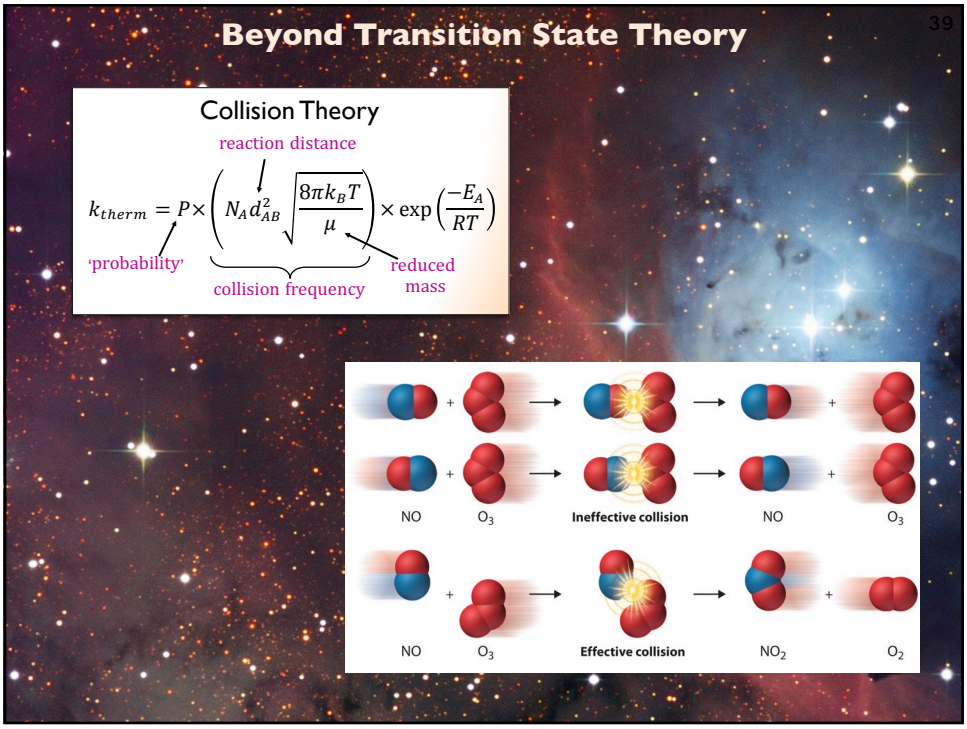

43

Beyond Transition State Theory

40

Tunnelling

- Quantum effect
- electrons, H^+ and $H\bullet$
- lower temperatures
- narrower barriers

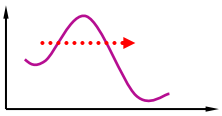

Tunnelling control of reaction

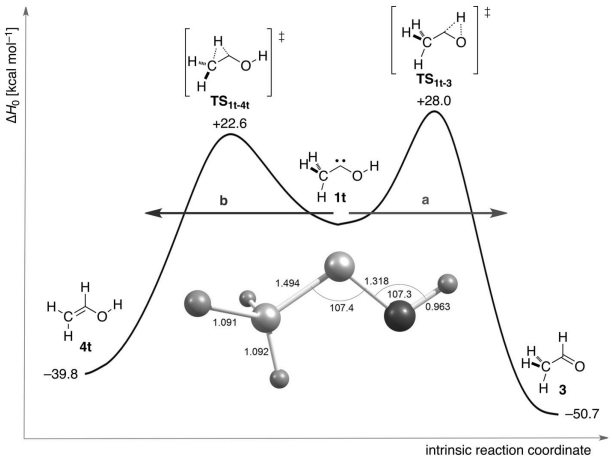

Without tunnelling at 11 K:
10^{100} times faster but still extremely slow ($k \approx 10^{-96}$ s^{-}

With tunnelling through narrower barrier: the only product

Schreiner, Allen et al., *Science*. **2011**, *332*, 1300.

44

Mini Quiz

1. Match kinetic profile of the initial steps of metathesis to the catalyst

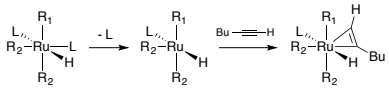

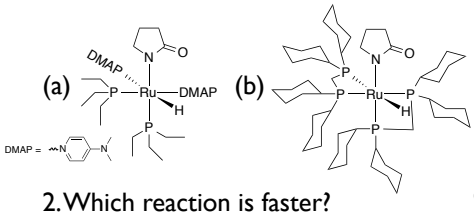

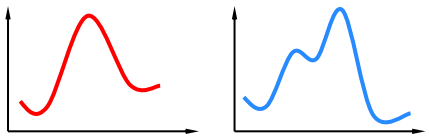

2. Which reaction is faster?
Which one is more exergonic?

(a) $\cdot CH_3$ + 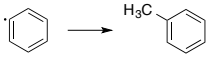

(b) $\cdot CH_3$ + 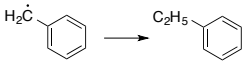

(c) $\cdot CH_3$ + 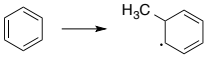

3. Match reaction sequence to the energy profile

(a) $A \xrightarrow{+B} C \rightleftharpoons D$

(b) $2A\bullet \longrightarrow C \underset{-B}{\longrightarrow} D$

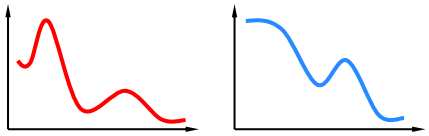

45